Metrol. Meas. Syst., Vol. XXI (2014), No. 2, pp. 257–270.

METROLOGY AND MEASUREMENT SYSTEMS

Index 330930, ISSN 0860-8229

www.metrology.pg.gda.pl

AN ON-SITE CALIBRATION SYSTEM FOR ELECTRONIC INSTRUMENT TRANSFORMERS BASED ON LABVIEW

Ming Zhang [1)], **Kaicheng Li** [2)], **Jun Wang** [1)], **Shunfan He** [2)]

1) Wuhan Textile University, School of Electronic and Electrical Engineering, Wuhan 430074, Hubei Province, China (✉zhangming@wtu.edu.cn)

2) Huazhong University of Science and Technology, School of Electrical and Electronic Engineering, Wuhan 430074, Hubei Province, China

Abstract

Electronic voltage transformers (EVT) and electronic current transformers (ECT) are important instruments in a digital substation. For simple, rapid and convenient development, the paper proposed an on-site calibration system for electronic instrument transformers based on LabVIEW. In the system, analog signal sampling precision and dynamic range are guaranteed by the Agilent 3458A digital multimeter, and data synchronization is also achieved based on a self-developed PCI synchronization card. To improve the measurement accuracy, an error correction algorithm based on the Hanning window interpolation FFT has good suppression of frequency fluctuation and inter-harmonics interference. The human-computer interface and analysis algorithm are designed based on LabVIEW, and the adaptive communication technology is designed based on IEC61850 9-1/2. The calibration system can take into account pairs of digital output and analog output of the electronic voltage/current transformer calibration. The results of system tests show that the calibration system can meet the requirements of 0.2 class calibration accuracy, and the actual type test and on-site calibration also show that the system is easy to operate with convenience and satisfactory stability.

Keywords: calibration system, electronic instrument transformers, data acquisition , data synchronization, LabVIEW.

1. Introduction

In recent years, with the rapid development of substation automation and network communication technology, especially the promulgation and implementation of the IEC 61850 standard, the traditional substation has shown gradual transition to a digital substation.

Electronic voltage transformers (EVT) and electronic current transformers (ECT) are important instruments in digital substations [1-3]. Their outputs are sent to the merging unit (MU) of transformers, and digital signals are converted into the data bus serving for substation monitoring, relay protection and control systems, so reliability can reach 99%. Based on the IEC60044-7/8 standards, the electronic transformer secondary output is divided into two kinds of digital output and analog output [4-5]. However, traditional calibration equipment cannot meet the requirements. This motivates some study of calibration systems of electronic instrument transformers [6-9].

Calibration systems with digital output and analog output are used to replace conventional calibration systems because of the principle of diversity and characteristics of EVT/ECT. Therefore mainly considering the factors influencing the accuracy of the calibration system and employing a simple but reliable structure, an on-site calibration system for electronic instrument transformers is designed with a rated voltage of 10 to 500 kV of EVT and a rated current of 5 to 5000 A of ECT. In the system, an Agilent 3458A digital multimeter is used to

Article history: received on Jan. 16, 2013; accepted on Nov. 22, 2013; available online on may. 15, 2014; DOI: 10.2478/mms-2014-0022.

greatly expand the sampling precision to improve the accuracy and reliability. For data acquisition to obtain simultaneous measurements, the self-developed PCI synchronization card can provide pulse synchronization signals to synchronize the reference and tested channels of the system. The human-computer interface and analysis algorithm are designed based on LabVIEW, which can make a real-time display of the waveform, frequency, amplitude, phase, and other data to facilitate comprehensive analysis of transformer performance. On the other hand, software exploiting, debugging and improving are easier, compared with the hardware circuit. It not only accelerates progress in the development, but also improves the stability of the product [10-11]. The system has achieved a high accuracy of EVT/ECT calibration, which enhances both the flexibility of digital signal processing and the computing speed as well. To improve the measurement accuracy, the Hanning window interpolation FFT (HWIpFFT) algorithm is used. It not only meets the requirements of high-precision sampling, but also is not sensitive to high frequency interference and frequency fluctuation of the tested signal.

The combination of the key technologies which were proposed in the paper is the most important feature to realize high accuracy and also the contributions of the paper. The paper is organized as follows. Section 2 elaborates the theory and design proposal of the system. The design of the on-site calibration system is presented first and then the scheme of the key technologies is discussed in Section 3. Then experiment results are presented and discussed in Section 4. At last, the conclusions are given in Section 5.

2. Principle and structure

In this paper, according to the IEC 60044-7/8 standard, the on-site calibration system of electronic instrument transformers is designed to estimate the measuring accuracy of the tested EVT/ECT. The block diagrams of the calibration system are shown in Figs. 1 and 2. They describe the system principle and structure of testing of EVT/ECT, respectively.

The proposed calibration system contains a reference channel, a tested channel, and a testing device. In Fig. 1, the reference channel includes the standard voltage transformer (VT), and $8\frac{1}{2}$ digital multimeter (Agilent 3458A for analog-to-digital conversion). In Fig. 2, the reference channel includes the standard current transformer (CT), sampling resistor, and Agilent 3458A. The standard CT would provide an output current, and then through the sampling resistor, the Agilent digital multimeter with data acquisition functions can acquire the signal and ensure high accuracy. In Figs. 1 and 2, the tested channel includes the tested EVT/ECT and MU. The signal from the tested EVT/ECT is sampled on the high voltage side of power systems, then sampling results are transmitted to the MU by the optical fiber.

The data reception of the reference and tested channels is charged by the testing device based on an industrial personal computer (IPC), which has a PCI-GPIB (general purpose interface bus) card and an Ethernet interface. Using a self-developed clock synchronization card, the IPC transmits pulse synchronization signals to achieve the synchronization of data acquisition. Then, the IPC begins receiving 10 cycles of data from the two channels every time and stores them in order. In the IPC, Labview is used as the unified software platform for computing, saving, calling, and displaying, which provides a convenient way for the proposed calibration system. Thus, the development program is characterized by the use of software to calibrate the tested EVT/ECT with the standard transformer. A number of measurements can be performed, for example ratio error, phase error, frequency, harmonic content about two sets of data using the HWIpFFT algorithm.

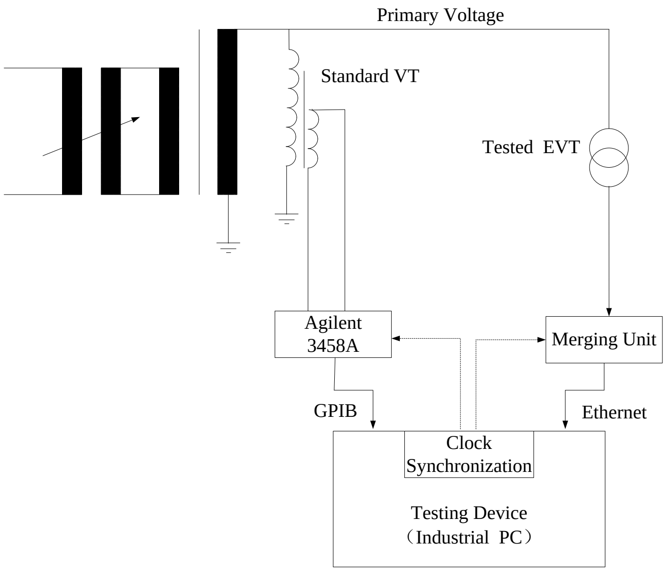

Fig. 1. Block diagram of the calibration system for testing EVT.

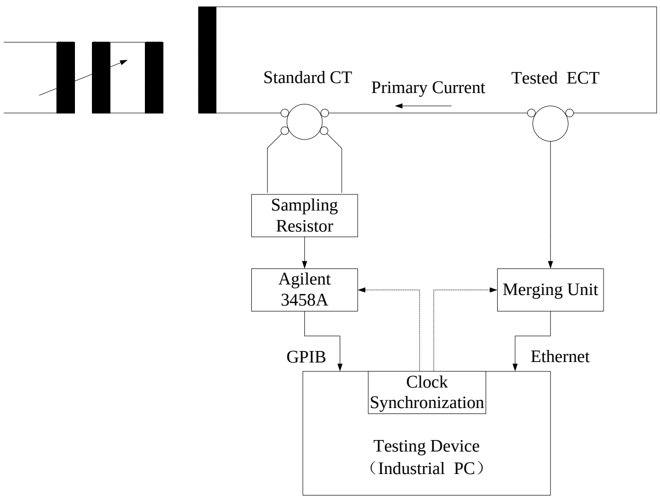

Fig. 2. Block diagram of the calibration system for testing ECT.

3. Design

Furthermore, the proposed calibration system combines the signal conversion unit, data acquisition unit, signal synchronization unit, IPC, and LabVIEW software programs and so on. In the system, signal acquisition, signal synchronization and other hardware are concentrated in an IPC in which signal processing and other functions are implemented by the Labview software.

3.1. Hardware Design

(1) Signal conversion unit (I/V conversion). The unit is individually set for CT calibration. The secondary current output signals of the standard CT (with accuracy 0.02 class) are converted to voltage signals by the high precision sampling resistor (1Ω with 0.01 accuracy class), so that the Agilent digital multimeter can read data properly.

(2) Data acquisition unit. The Agilent 3458A digital multimeter is the fastest, most flexible, and most accurate multimeter offered by Agilent Technologies, which is important to be compatible with LabVIEW software. It is used to measure the input signals as an A/D converter of the reference channel. It can provide an effective precision of 24 bits with the least significant bit weighted 2^{-23}. The error of the test setup is small enough to be ignored when it is used for verification of the calibration. MUs are used to merge and synchronize the sampled voltage/current signals and transmit these data to IEDs (intelligent electronic devices). The model of the MU used in the paper is OEMU702. It supports connectons to EVT/ECT and electro-magnetic VT/CT. And it can also operate as an A/D and D/A converter in a substation between the ECT/EVT and conventional VT/CT to deliver synchronized signals to busbar protection and transformer protection. The technical data of OEMU702 is shown in Table 1.

Table 1. Technical data of OEMU702.

Merging Unit	**OEMU702**
Rated DC power	220V/110V
Rated DC output	+5V/10A
Number of inputs (PPL)	9
Sampling rate (for 50 Hz)	4000 Hz
Rated delay time	$3T_s$ (T_s is the sampling cycle)
Measurement accuracy	0.2S
Protection accuracy	5P
Communication interface	10Base-T/100Base-TX, RS-485, RS-232
Working temperature range	-10～50℃
Standards	IEC60044-7/8, IEC61850-9-1/2

(3) Signal synchronization unit. The key of the calibration system is also reflected on the pulse synchronization signals. The acquisition process must be synchronized sampling, or else the calculation results will lack any sense. The PCI synchronization card is self-developed, based on the ARM7 microcontroller (LPC2214). The synchronization error limit can be less than ± 1μs if each MU shall be able to compensate the signal delay. The card is inserted in the IPC PCI slot, and can output four synchronous pulses of the 2-channel electrical signals and 2-channel optical signals. So, it is easy to be used to meet the different synchronization needs of MUs. The block diagram of the PCI synchronization card is shown in Fig.3. As shown in Fig.3, we design a serial port in the card, which is for serial communication between the PCI synchronization card and IPC. It can be convenient and flexible to use a different PC.

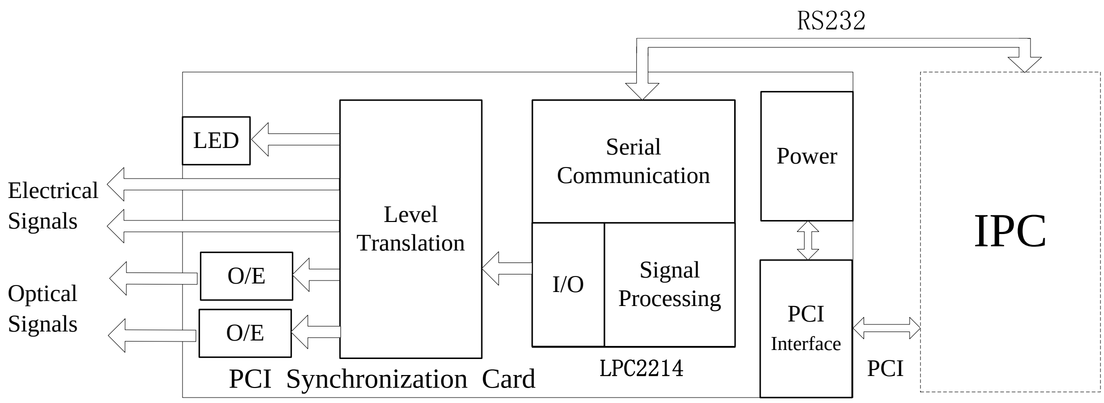

Fig. 3. Block diagram of the PCI synchronization card.

In the tests, the MU and Agilent 3458A must reach time synchronization for the calibration [12-13]. Therefore, the IPC uses a clock synchronization signal to control synchronous sampling of the two channels. The two channels start sampling when they receive the synchronizing pulse generated by the synchronization card. The optical synchronization pulse signal (or electrical synchronization pulse signal) is used for the MU clock synchronization, so that the sampling beats of the MU are synchronous with Agilent 3458A. So, this will confirm the synchronization of the signals that are from the reference and tested channels, and it can make sure that the follow-up analysis is correct.

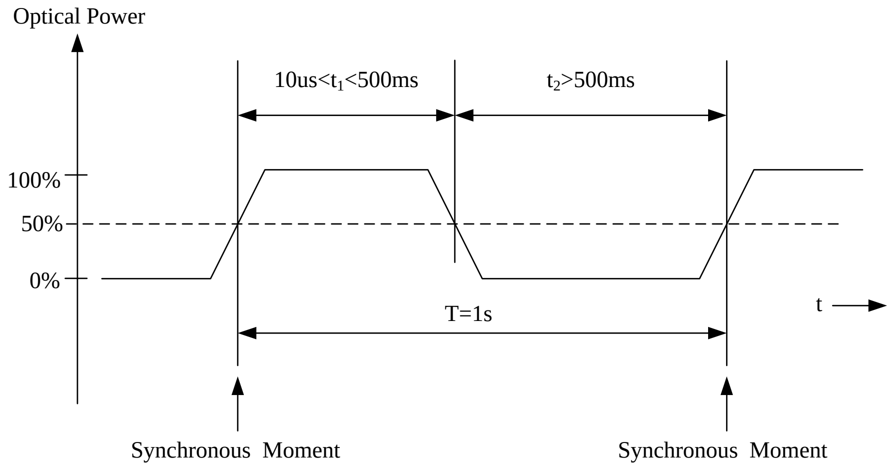

Fig. 4. Synchronization second pulse signal waveform.

Fig.4 shows the technical requirements of the synchronization second pulse signal. The clock frequency is 1 Hz. The triggering optical power is 50% of the maximum optical power at the rising edge of synchronization second pulse signal. Generally the MUs can detect the correctness of the signal. If the difference between adjacent pulses interval time and the ideal interval time (1s) is larger than 10μs, the synchronization signal is abnormal, then the synchronization state sent out according to IEC61850-9 is “1”. Otherwise, the MUs can be synchronized and send out the synchronization state as “0” according to IEC61850-9.

(4) Interfaces. The GPIB interface and Ethernet interface can improve reliability and convenient access interface of the calibration system. And high-speed data transfer can be carried out by these interfaces in the system too. The NI PCI-GPIB communication card is used , inserted in the IPC PCI slot. It can facilitate the connection between the IPC and Agilent 3458A. Further, it is important that LabVIEW software supports GPIB and Ethernet protocols.

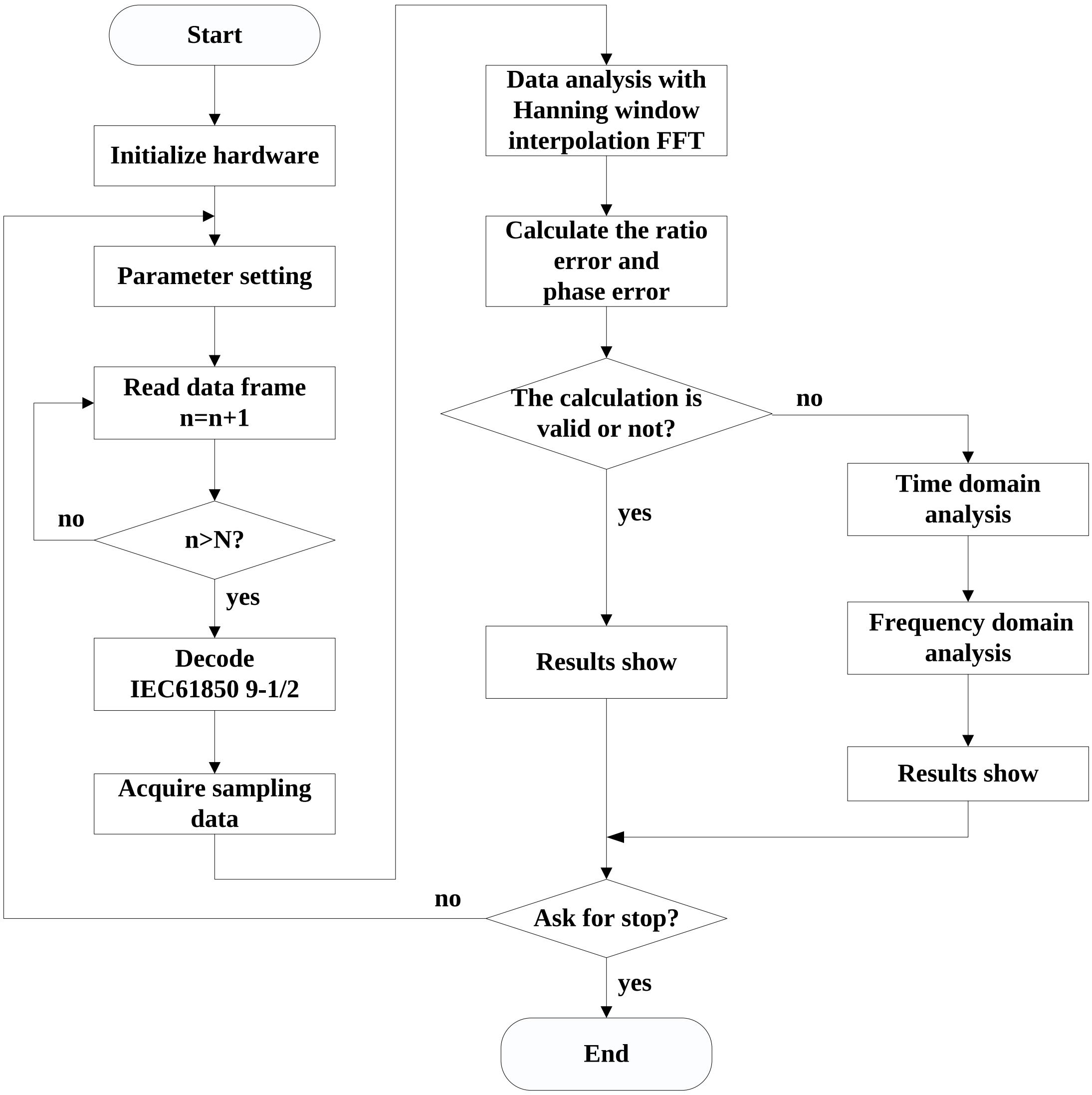

Fig. 5. Software flowchart of the calibration system.

3.2. Software design

3.2.1. Calibration software design

The calibration software is used to mainly perform two tasks: the communication between the IPC and local instruments, and data analysis. The software flowchart is shown in Fig. 5.

The calibration system interface is designed by LabVIEW software, and software interface consists of three parts: parameter setting interface, data analysis interface and parameter analysis interface.

Parameter setting interface shown in Fig. 6 is to complete calibration parameters setting, including digital/analog transformer selection, system rated primary/secondary value setting, systems protocol selection, calibration channel selection and calibration times.

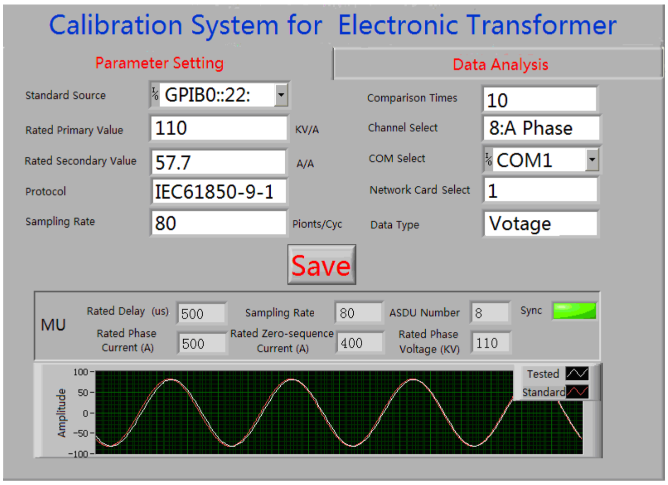

Fig. 6. Parameter setting interface of the calibration system.

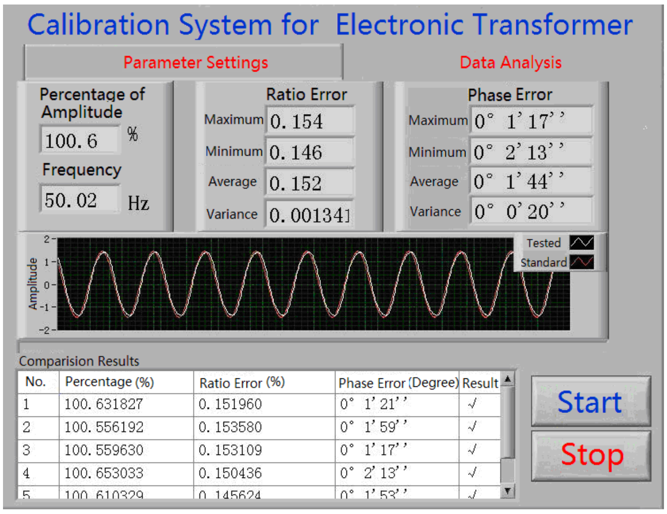

Fig. 7. Data analysis interface of the calibration system.

Data analysis interface is mainly to show the calculating results, shown in Fig.7. The interface is the core of the system. After parameters setting is completed, click the "Start" button ("one-button" model) to complete the whole measurement and calibration process in accordance with configuration parameters, and be able to display the percentage of the standard source amplitude, system frequency, ratio errors (max, minimum and average), phase errors (maximum, minimum and average), real-time waveforms, progress of the implementation of system test, detailed list of parameters (percentage of amplitude, ratio error, phase error) and calculation is valid or not for each comparison, etc..

Parameter analysis interface is mainly for the failure calibration of the transformer, shown in Fig.8. In the time domain analysis, frequency, amplitude, phase angle, and other parameters of the two channels' signals would be calculated. For the frequency domain analysis, it can automatically analyze the amplitude spectrum of the two channels' signals from DC, 2 to 20 harmonics, then calculate the harmonic ratio (HR), total harmonic distortion (THD) of them.

HR is the ratio of the amplitude of the kth harmonic to the amplitude of the first harmonic (fundamental frequency component). The HR is usually expressed in percent, for a voltage signal, which can equivalently be written as

$$HRU_{\mathrm{k}} = \frac{U_{\mathrm{k}}}{U_1}, \tag{1}$$

where U_{k} is the RMS (root-mean-square) voltage of the *k*th harmonic. U_1 is the RMS voltage of the first harmonic.

THD is defined as an amplitude ratio of the square root of all higher harmonic frequencies to the amplitude of the first harmonic. The THD is also usually expressed in percent, for a voltage signal, which can equivalently be written as

$$THD = \frac{U_{\mathrm{H}}}{U_1}, \tag{2}$$

where U_{H} is the square root of all higher harmonic frequencies, given by

$$U_{\mathrm{H}} = \sqrt{U_2^2 + U_3^2 + \cdots + U_k^2 + \cdots} = \sqrt{\sum_{k=2}^{N} U_k^2}.$$

At last, the results of time domain and frequency domain analysis are shown to facilitate a comparative analysis of transformer performance.

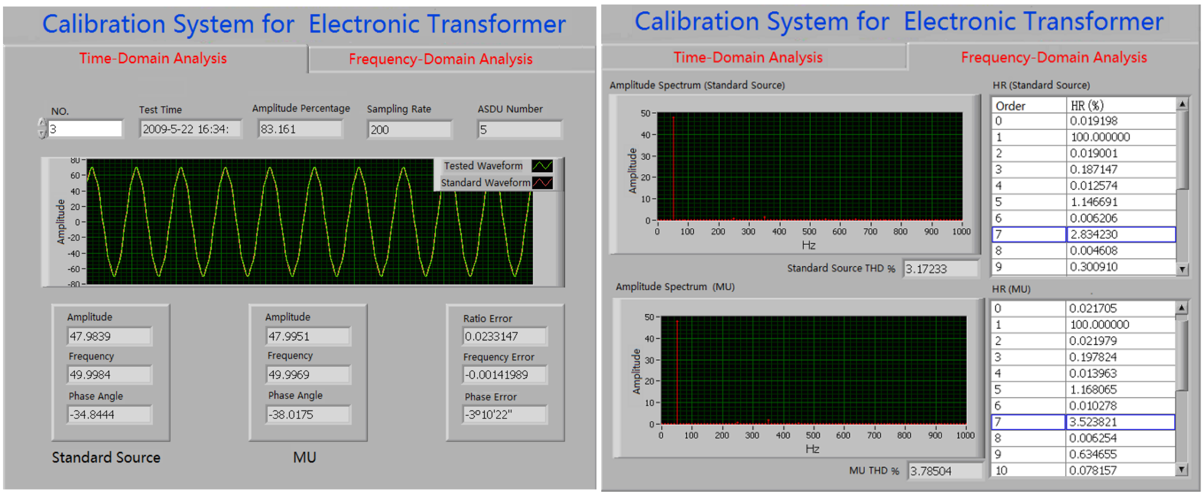

(a) (b)

Fig. 8. Parameter analysis interface of the calibration system. (a) Time domain analysis interface. (b) Frequency domain analysis interface.

3.2.2. System communication

System communication refers to communication between the calibration system and the MU. With the strong construction of the digital substation, the communication protocol of the MU tends to be standardized using the IEC 61850-9 standard [12-13]. In the software design of the calibration system, it is compatible with three protocols { IEC61850 (-9-1, -9-2,-9-2LE) }. So, the system can be flexible to select the communication protocol to calibrate the electronic instrument transformers with various communication modes, and provide full frame resolution to automatically analyze ASDU (application service data unit) data.

3.2.3 Error calculation algorithm with HWIpFFT

As it is well known, actual power signals are not ideal. They can be considered as the sum of a series of different components superimposed over a fundamental component, and the amplitude of a harmonic is generally a few percent of that of the fundamental or smaller.

When non-synchronous sampling is done on the actual signal, the spectrum leakage will seriously affect the fundamental frequency component by the FFT, resulting in great error of the calibration system. And the large-amplitude harmonic components also can overwhelm the small ones. An appropriate window function and interpolation algorithm can improve the accuracy of the FFT.

Interpolation FFT(IpFFT) is a well known technique that allows improving the parameter estimation accuracy of a non-synchronous sampling signal. By convoluting the used window function spectrum with a non-synchronous sampling signal, a theoretical function for the expected spectrum of the FFT peaks is obtained. Thus interpolating the FFT peaks with this function will result in improved parameter estimation. For real-time use, the algorithm must have a tradeoff between accuracy and execution time. In this paper, the selected IpFFT algorithm is a two-point algorithm using the Hanning window [14].

Consider a sampled monofrequency signal

$$x(k\Delta t) = A\sin(2\pi fk\Delta t + \phi) \ , \tag{3}$$

where $k = 0,1,2,\cdots,N-1$, f is the frequency, A is the amplitude, ϕ is the phase angle, and Δt is the sampling interval. For simplicity, a scaled frequency is used as

$$f = (L+\delta) f_0 = \lambda f_0, \quad f_0 = \frac{1}{N\Delta t} \ , \tag{4}$$

with L the integer part of λ and δ the fractional part of λ. Eq.(3) is rewritten as

$$x(k) = A\sin(2\pi\lambda \frac{k}{N} + \phi) \ . \tag{5}$$

The FFT of this signal at spectral line k_1 is given by

$$X(k_1) = 0.5(Ae^{j\phi}W((\lambda - k_1) f_0) + Ae^{j\phi}W((\lambda + k_1) f_0)), \tag{6}$$

where $W(f)$ is the spectrum of the selected time-domain window.

As shown in Fig.9, including the spectral line with the maximum amplitude, the IpFFT algorithm uses an estimation scheme with two spectral lines ($X(k_1), X(k_1+1)$), and subsequently calculates the corresponding parameters of the spectral line ($X(k_1+0)$ or $X(k_1+0.5)$).

For the Hanning window, an approximate solution is

$$\alpha = \frac{|X_H(k_1+1)|}{|X_H(k_1)|}, \ \delta_1 = \frac{2\alpha - 1}{\alpha + 1}, \ f_1 = (k_1 + \delta_1) f_0,$$

$$A_1 = |X_H(k_1)| \frac{[2\pi\delta_1(1-\delta_1^2)]}{\sin(\pi\delta_1)}, \tag{7}$$

$$\phi_1 = angle(|X_H(k_1)|) - \delta_1\pi(N-1)/N \ .$$

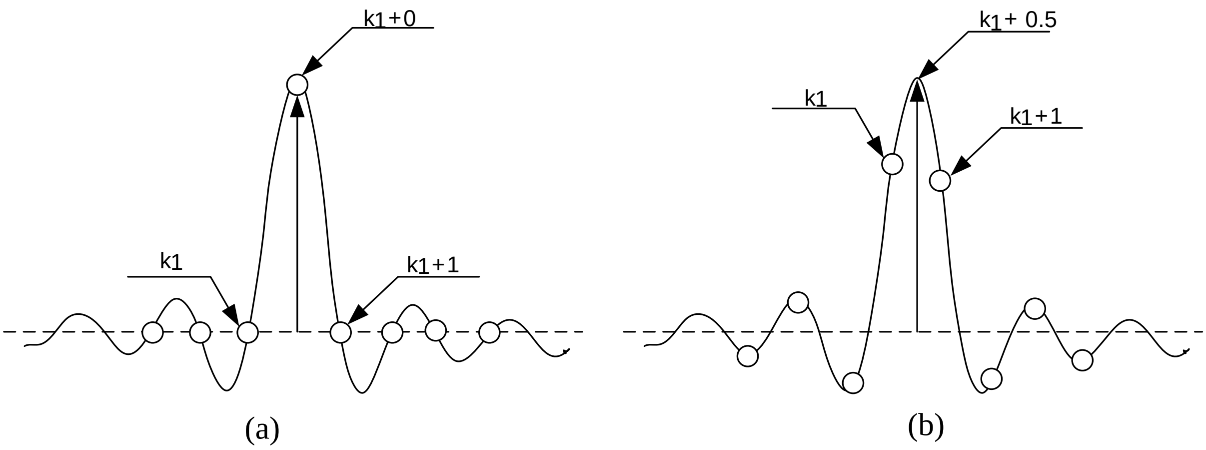

Fig. 9. Interpolated discrete Fourier transform. (a) $\delta_1 = 0$. (b) $\delta_1 = 0.5$.

3.3 Uncertainty of the system

There are three main factors of uncertainty of the calibration system: the standard VT/CT, the digital sampling system and the error calculation method.

The standard VT/CT uncertainty can be measured by comparing with a much more accurate reference transducer. The uncertainty of the standard VT is found to be less than 0.01% for ratio error and 0.2 min for phase error. The uncertainty of the standard CT is less than 0.02% for ratio error and 0.3 min for phase error. The sampling resistor is used as the rated secondary burden of the standard CT and as the converter from current to voltage which supplies the Agilent 3458A with proper voltage value. The resistor was tested by the precision impedance analyzer. The relative error of the resistance is less than 0.01%.

The calibration system requires not only high resolution but also low uncertainty. To assure low uncertainty, the Agilent 3458A digital multimeter is used. It can achieve low-uncertainty performance with 100 ppm best accuracy for AC voltages. And it has the digital sampling function and external trigger synchronous sampling mode, which can ensure sampling accuracy (signal amplitude) and sampling synchronization (signal delay). The quantization error and nonlinearity error of the AD converters in the Agilent 3458A can be neglected since their effects are usually negligible[15].

Leakage effects happen when the sampling rate is not an exact multiple of the frequency of the voltage or current that is applied to the primary of the reference and tested transformers. The windows technique and phase difference correction method can greatly reduce the effects. Thus the HWIpFFT algorithm can analyze the signals with very high accuracy, which is normally less than 0.05%[14].

4. Experiment

4.1. Definitions for the error calculation

Take the EVT testing for example. In order to individually verify the tested EVT, its accuracy can be measured in a large range of voltages by comparing it to the standard VT with an accuracy of class 0.02. The ratio error ε_u is defined as [4]

$$\varepsilon_\mathrm{u}(\%) = \frac{K_\mathrm{n} U_\mathrm{s} - U_\mathrm{p}}{U_\mathrm{p}} \times 100 \;, \tag{8}$$

where K_n is the rated transformation ratio, U_p is the (RMS) value of the primary voltage, U_s is the RMS value of the secondary voltage. The general definition for the phase error ϕ_u is

$$\phi_u(\mathrm{rad}) = \phi_\mathrm{s} - \phi_\mathrm{p} \,, \tag{9}$$

where ϕ_p is the phase angle of the primary voltage, ϕ_s is the phase angle of the secondary voltage.

ECT testing is performed in the same way as the EVT testing[5].

4.2. Type test

In order to test the correctness of the calibration system, the following tests are done in the laboratory. A FLUKE 5720A multifunction calibrator as a standard signal source combines with the calibration system to measure the ratio error and phase error, which can provide two standard voltage signals. The calibration schematics of ratio error and phase error measurement are shown in Fig.10, respectively.

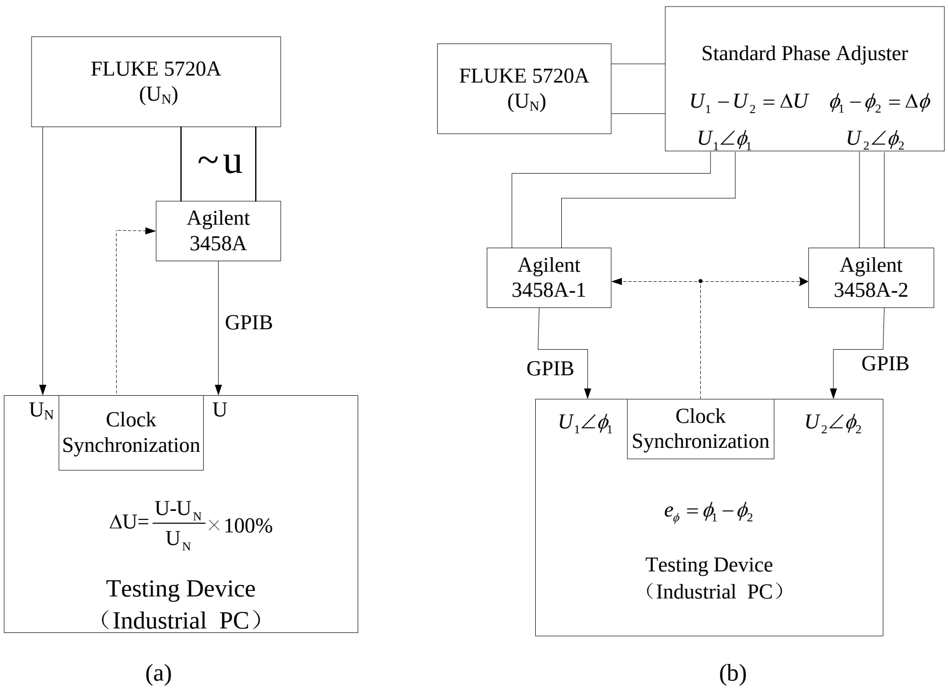

Fig. 10. The calibration schematics of (a) ratio error measurement and (b) phase error measurement.

Measurement results show that the calibration system can achieve 0.05% accuracy. So, the system can meet the requirements of 0.2 class calibration accuracy of electronic instrument transformers.

4.3. On-site calibration

According to Figs.1 and 2, we have set up a calibration system which is specified to verify accuracy and feasibility of the tested EVT/ECT. This system has been used for on-site calibration in the Sanxiang substation in Guangdong province, shown in Fig.11.

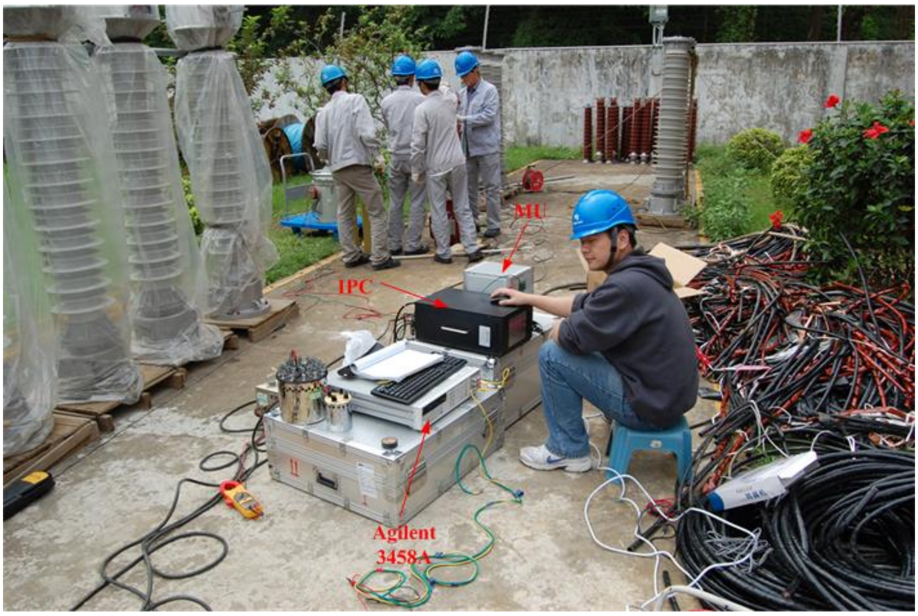

Fig. 11. The picture of on-site calibration in Sanxiang substation.

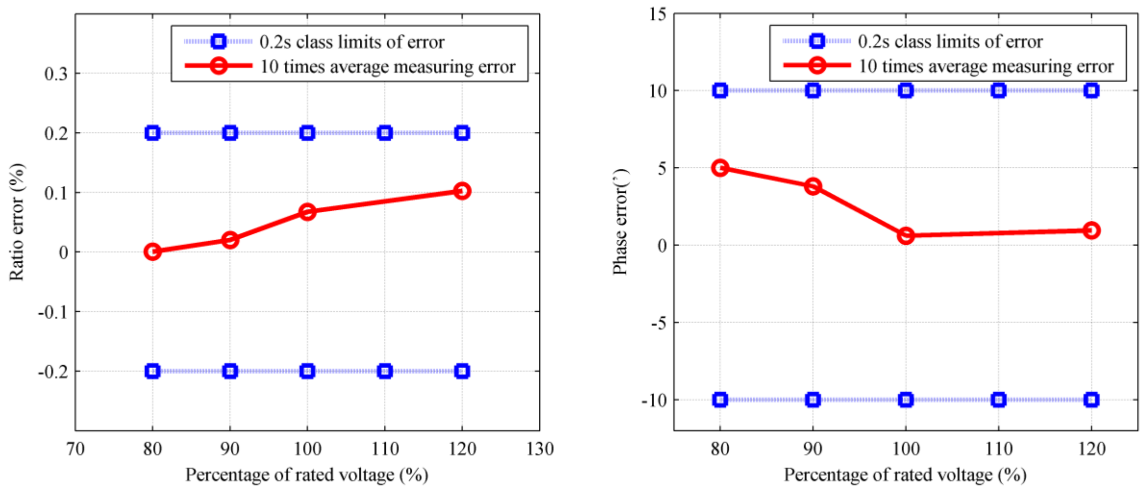

(a) (b)

Fig. 12. (a) Percentage ratio error results of the tested EVT . (b) Phase error results of the tested EVT.

In the actual tests, 10 samples in each data point are adopted in the error calculation procedure. According to IEC60044-7, voltage at the 80%～120% of rated voltage must meet the accuracy requirements for the tested EVT. Test results are shown in Fig.12 (transformer type: EVT; test channel: A phase; rated transformation ratio of measuring voltage:

10 kV/57.7V; test times: 10; transformer inherent delay: 255μs). According to IEC60044-8, current at the 5 ~ 120% of rated current must meet the accuracy requirements for the tested ECT. Test results are shown in Fig.13 (transformer type: ECT; test channel: A phase; rated transformation ratio of measuring current: 300A/1A; test times: 10; transformer inherent delay: 188μs).

As shown in Figs.13 and 14, the percentage ratio error and phase error of the tested 0.2 class EVT/ECT are small and lower than the 0.2s class limit. So, the EVT/ECT can meet the accuracy requirements of a 0.2 class standard.

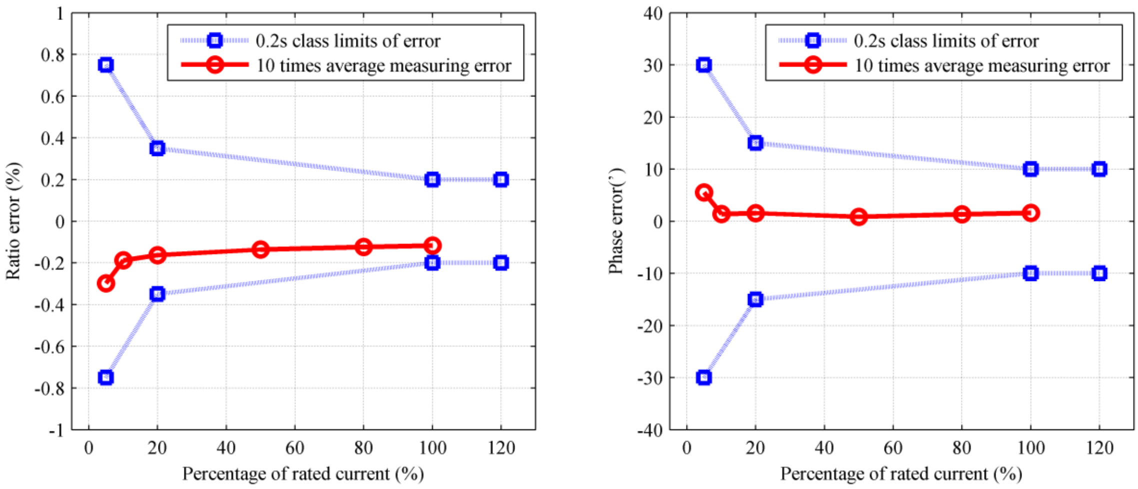

(a) (b)

Fig. 13. (a) Percentage ratio error results of the tested ECT .
(b) Phase error results of the tested ECT.

5. Conclusions

In this paper, an on-site calibration system for electronic voltage and current transformers with both analog and digital outputs has been introduced. The signals are measured at the secondary outputs of the reference transformer and tested transformer when the same excitation signal is fed to their primaries. To improve the measurement accuracy, the HWIpFFT algorithm is used. Labview is used as the unified software platform for computing, saving, calling and displaying, which provides a convenient way for the proposed calibration system. In accordance with IEC60044-7/8, the system can verify the ratio error and phase error of the tested EVT/ECT.

The type test results mentioned above show that the proposed system has a high accuracy qualified to the calibration of the tested EVT/ECT. The on-site calibration proves that it is also convenient in the on-site installation and implementation. The experiment results show that it can meet the calibration requirements of the electronic instrument transformer with 0.2s class. So, the system is suitable for on-site testing due to its high accuracy, simple structure and low-cost hardware.

Acknowledgments

This work was supported by Natural Science Foundation of China grants 51077058 and 51277080.

References

[1] Kang, M.(1999). Analysis and design of electronic transformers for electric power distribution system. *IEEE Trans. Power Electron.*,14(6),1133–1141.

[2] Chen, Q., Li, H. B., Huang, B.X. (2010). An innovative combined electronic instrument transformer applied in high voltage lines. *Measurement*, 43 (7) ,960–965.

[3] Faifer, M., Toscani, S., Ottoboni, R. (2011). Electronic combined transformer for power-quality measurements in high-voltage systems. *IEEE Trans. Instrum. Meas.*, 60 (6), 2007–2013.

[4] IEC60044-7 (2002). *Instrument Transformer-part 7, Electronic Voltage Transformers*. International Electrotechnical Commission: Geneva, Switzerland.

[5] IEC60044-8 (2002). *Instrument Transformer-part 8, Electronic Current Transformers*. International Electrotechnical Commission: Geneva, Switzerland.

[6] Brandolini, A., Faifer, M., Ottoboni, R. (2009). A simple method for the calibration of traditional and electronic measurement current and voltage transformers. *IEEE Trans. Instrum. Meas.*, 58(5),1345–1353.

[7] Djokic, B. (2010). Calibration of Rogowski coils at frequencies up to 10 kHz using digital sampling. *IEEE Trans. Instrum. Meas.*, 59 (5), 1303–1308.

[8] Tong, Y., Ye, G. X., Guo, K. Q., Li, H. B. (2011). Highly accurate calibration system for electronic instrument transformers. *Metrol. Meas. Syst.*, XVIII (2), 315–322.

[9] Zhang, Z., Li, H. B. (2012). An accurate system for onsite calibration of electronic transformers with digital output. *Rev. Sci. Instrum.*, 83 (6), 065111:1–7.

[10] Winiecki, P. W.(2002). Virtual spectrum analyzer based on data acquisition card. *IEEE Trans. Instrum*. Meas., 51(1), 82–87.

[11] Bo, L., Liu, X. F., He, X. X. (2011). Measurement system for wind turbines noises assessment based on LabVIEW. *Measurement*, 44 (2) ,445–453.

[12] IEC 61850-9-1 (2003). *Communication Networks and Systems in Substations—Part 9-1: Specific Communication Service Mapping (SCSM)—Sampled Values over Serial Unidirectional Multidrop Point to Point Link*. International Electrotechnical Commission: Geneva, Switzerland.

[13] IEC 61850-9-2 (2004). *Communication Networks and Systems in Substations—Part 9-2: Specific Communication Service Mapping (SCSM)—Sampled Values over ISO/IEC 8802-3*. International Electrotechnical Commission: Geneva, Switzerland.

[14] Zhang, M., Li , K. C., Hu, Y. S. (2011). A high efficient compression scheme for power quality applications. *IEEE Trans. Instrum. Meas.*, 60(6) ,1976–1985.

[15] Agilent Technologies (2000). *Agilent Technologies 3458A Multimeter User's Guide*. Agilent Technologies Inc..